Mathematics Notes

Note 99

July 2, 2008

A Correction Procedure for Corrupted Measured Spectra

F. M. Tesche
Holcombe Dept. of Electrical and Computer Engineering
College of Engineering & Science, 337 Fluor Daniel Building
Box 340915, Clemson, SC 29634-0915

Abstract

This note investigates the feasibility of using an integral equation technique based on the Hilbert transform to correct a non-causal spectrum over a limited band of frequencies. Assuming that a computed or measured spectrum is causal outside of a given frequency band, a set of 2 coupled integral equations have been formulated and solved for the unknown real and imaginary parts of the spectrum within the band. For these equations, the forcing functions are integrals of the known spectrum. Details of the formulation of this method and two numerical examples are provided

---

This work was supported by the Swiss Defense Procurement Agency of the Federal Department of Defense, Civil Protection and Sports.

Contents

A Correction Procedure for Corrupted Measured Spectra

1. Introduction

In performing wideband electrical testing of electronic systems, it is common to encounter spectral (frequency domain) data that are partially corrupted by noise. The presence of this noise can lead to difficulties in processing these data and in obtaining a meaningful interpretation of the measured responses.

As discussed in an IEC Standard for HEMP test procedures [1], measurements can be conducted in either the time or frequency domain. As noted in Figure 1, which is a block diagram illustrating the use of transient measurements for determining the frequency domain transfer function or shielding effectiveness of an enclosure, there is a step in the process which involves dividing an internal response spectrum $R(\omega)$ by an external excitation function $F(\omega)$ to obtain a transfer function $T(\omega)$ as

$$T(\omega) = \frac{R(\omega)}{F(\omega)} \tag{1}$$

Since the measurements are conducted in the time domain for this example, the spectral components $R(\omega)$ and $F(\omega)$ are computed by taking the Fourier transforms of the measured transient data. As described in a well-known reference on the Fourier transform [2], a function of time $f(t)$ can be decomposed into a superposition of many different sinusoidal waveforms, each having a distinct amplitude and phase. There are several different forms for this expression [3], one of which is the exponential form:

$$f(t) = \frac{1}{2\pi} \int_{-\infty}^{\infty} F(\omega) \exp(j\omega t) d\omega \quad , \tag{2a}$$

where the spectral density $F(\omega)$ is a complex-valued function that represents the amplitude and phase of a sinusoidal waveform component given by the phasor $\exp(j\omega t)$. This spectrum may be determined from knowledge of the time function through the inverse Fourier transform relation,

$$F(\omega) = \int_{-\infty}^{\infty} f(t) \exp(-j\omega t) dt \quad . \tag{2b}$$

Normally, the evaluation of Eq.(1) to determine the transfer function $T(\omega)$ is a simple task, and it proceeds without difficulty. However, occasionally the excitation spectrum $F(\omega)$ may decrease in amplitude to the point that the system noise level masks its actual value. Such cases arise when there can be destructive interference in wave paths, for example. In this case, the ideal transfer function would be undefined; however, with the presence of noise in the measurement, there can be a large, artificial resonance introduced into the computed transfer function spectrum. Removing this artifact in the transfer function is the goal of this work.

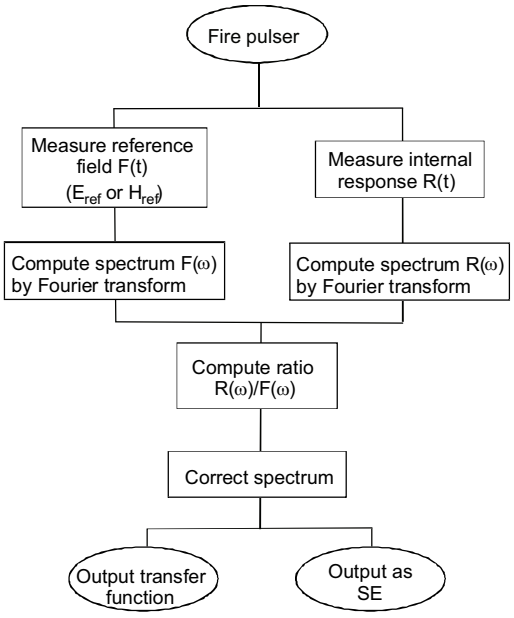

Figure 1. Block diagram of the use of transient measurements to determine the frequency domain transfer function or shielding effectiveness of an enclosure.

This difficulty with calculating an incorrect transfer function spectrum is not limited to the processing of measured transient data. It can arise with continuous wave (CW) measurements, as well. As described in [4], measured CW data representing the EM fields inside and outside of a shielding enclosure can be used to calculate the transient response for a specified transient external waveform. The details of this procedure are given in Figure 2, and once again, it is seen that a transfer function $T(\omega)$ is constructed from a ratio of two measured quantities, and this can lead to errors when the excitation spectrum E(w) is below the measurement noise.

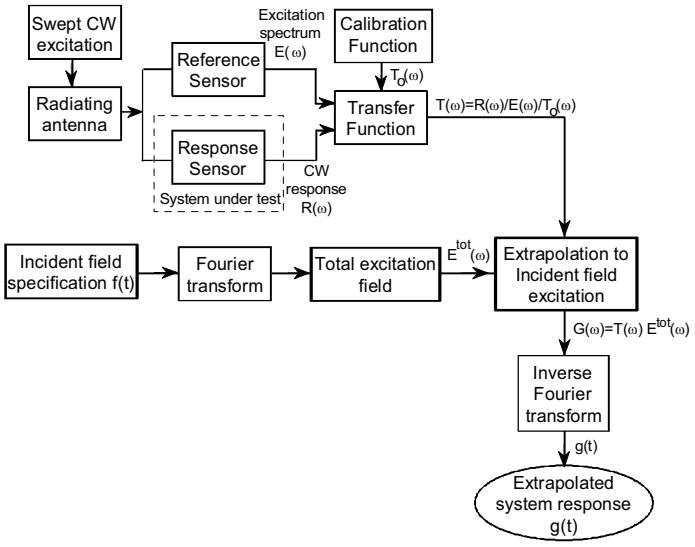

Figure 2. Block diagram of the CW data processing procedure.

In this report, we will investigate a method of correcting a computed transfer function having a small band of frequencies in which the value of the function is questionable. Such a spectrum is shown in Figure 3, which depicts a corrected transfer function obtained by processing measured CW data.

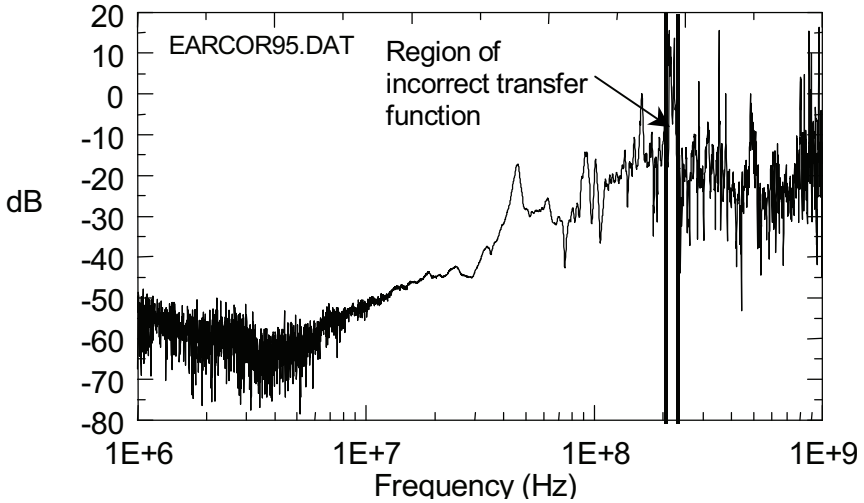

Figure 3. Illustration of a measured transfer function magnitude $|T(\omega)|$ having a region in which the value of the function is incorrect.

For performing this correction, a fundamental assumption that we make is that the transfer function $T(\omega)$ represents a *causal* transient response. As discussed in [5], this implies that the real and imaginary parts of $T(\omega)$ must satisfy the Hilbert transform relationships. In this reference, a method of filtering such a spectrum to remove non-causal components is described. This involves processing both the real and imaginary parts of the spectrum to obtain a causal spectrum.

In the present study, however, we will concentrate on the correction of the spectrum only in the range of frequencies in which the spectrum is suspected of being incorrect. To do this, we will use the Hilbert transform relationships to develop an integral equation for the "corrected" spectrum in the frequency band. This results in a selective removal of the non-causal portion of the spectrum and will lead to an improved spectral representation of the transient response of the system being studied.

2. Formulation of the Hilbert Integral Equations

2.1 The Hilbert Transform

As discussed in [6] and [7] the Hilbert transform is a commonly used technique for relating the real and imaginary parts of a spectral response. It results from an application of the Cauchy residue theorem in complex variable theory and it may be expressed in both continuous and discrete forms. It is widely used in circuit analysis, digital signal processing, image reconstruction, and remote sensing. For a complex-valued spectrum represented as

$$F(\omega) = X(\omega) + \mathrm{j}Y(\omega) \tag{3}$$

the Hilbert transform relationships are expressed as integrals of the real and imaginary parts in the form

$$X(\omega) = \frac{2}{\pi}\int_0^{\infty} \frac{\xi\, Y(\xi)}{\omega^2 - \xi^2} d\xi + K \tag{4a}$$

$$Y(\omega) = -\frac{2\omega}{\pi}\int_0^{\infty} \frac{X(\xi)}{\omega^2 - \xi^2} d\xi\,. \tag{4b}$$

In Eq.(4a) the presence of the constant term K represents a delta function contribution to the transient waveform $f(t)$, and in the present analysis, we assume that this term is zero.

2.2 The Hilbert Integral Equation

As mentioned earlier, we assume that both the real and imaginary parts of the spectrum $X(\omega)$ and $Y(\omega)$ are known for all frequencies, except for a small band of frequencies in the range from ω_1 to ω_2. In this manner, Eqs.(4) can be written as

$$X(\omega) = \frac{2}{\pi}\int_{\omega_1}^{\omega_2} \frac{\xi\, Y(\xi)}{\omega^2 - \xi^2} d\xi + A(w) \tag{5a}$$

and

$$Y(\omega) = -\frac{2\omega}{\pi}\int_{\omega_1}^{\omega_2} \frac{X(\xi)}{\omega^2 - \xi^2} d\xi + B(\omega) \tag{5b}$$

In these equations, the terms $A(\omega)$ and $B(\omega)$ are known functions involving the Hilbert integrals of the spectral components from 0 to ω_1 and ω_2 to ∞. These are given by the expressions

$$A(\omega) = \frac{2}{\pi}\left(\int_0^{\omega_1} \frac{\xi\, Y(\xi)}{\omega^2 - \xi^2} d\xi + \int_{\omega_2}^{\infty} \frac{\xi\, Y(\xi)}{\omega^2 - \xi^2} d\xi \right) \tag{6a}$$

and

$$B(\omega) = -\frac{2\omega}{\pi}\left(\int_0^{\omega_1} \frac{X(\xi)}{\omega^2 - \xi^2} d\xi + \int_{\omega_2}^{\infty} \frac{X(\xi)}{\omega^2 - \xi^2} d\xi \right). \tag{6b}$$

Letting the value of ω in these equations lie within the range $\omega_1 \le \omega \le \omega_2$ it is possible to write the following set of coupled integral equations for $X(\omega)$ and $Y(\omega)$ with the terms $A(\omega)$ and $B(\omega)$ as forcing functions:

$$X(\omega) - \frac{2}{\pi} \int_{\omega_1}^{\omega_2} \frac{\xi\, Y(\xi)}{\omega^2 - \xi^2} d\xi = A(\omega) \tag{7a}$$

$$Y(\omega) + \frac{2\omega}{\pi} \int_{\omega_1}^{\omega_2} \frac{X(\xi)}{\omega^2 - \xi^2} d\xi = B(\omega) \tag{7b}$$

3. Solution of the Hilbert Integral Equations

The solution of the Hilbert integral equations (7) for $X(\omega)$ and $Y(\omega)$ for $\omega_1 \le \omega \le \omega_2$ can be accomplished using the method of moments. This is done by representing the unknown functions as piece-wise constant functions, and on substituting these currents into the integrals, a matrix equation for the unknown functions results. Useful in this process are the following integrals:

$$\int_a^b \frac{\xi}{(\omega+\xi)(\omega+\xi)} d\zeta = \frac{1}{2}\ln\left[\frac{(a-\omega)(a+\omega)}{(b-\omega)(b+\omega)}\right] \tag{8}$$

and

$$\int_a^b \frac{1}{(\omega+\xi)(\omega-\xi)} d\zeta = \frac{1}{2\omega}\ln\left[\frac{(a-\omega)(b+\omega)}{(a+\omega)(b-\omega)}\right] \tag{9}$$

Assuming that the spectrum $T(\omega)$ is defined at frequency points having a uniform separation Δ, as $\omega_i = \Delta\, i$, for $i = 1$ to $N_{\max}$, and that the unknown portion of the frequency spectrum consists of N_p points having the range of indices $n_1 \le i \le n_2$ (e.g., $N_p = n_2 - n_1 + 1$), the integral term in Eq.(7a) at a particular frequency ω_i can be approximated as

$$\begin{aligned} -\frac{2}{\pi}\int_{\omega_1}^{\omega_2} \frac{\xi\, Y(\xi)}{\omega_i^{\,2} - \xi^2} d\xi &\approx \sum_{\substack{j=n_1 \\ j\neq i}}^{n_2} -\frac{1}{\pi}\ln\left[\frac{(i-j-\frac{1}{2})(i+j-\frac{1}{2})}{(i-j+\frac{1}{2})(i+j+\frac{1}{2})}\right] Y(j\Delta) \\ &\equiv \sum_{\substack{j=n_1 \\ j\neq i}}^{n_2} a_{i,j} Y_j \end{aligned} \tag{10a}$$

Similarly, the integral term in Eq.(7b) is approximately given as

$$\begin{aligned} \frac{2\omega_i}{\pi}\int_{\omega_1}^{\omega_2} \frac{X(\xi)}{\omega_i^{\,2} - \xi^2} d\xi &\approx \sum_{\substack{j=n_1 \\ j\neq i}}^{n_2} \frac{1}{\pi}\ln\left[\frac{(i-j-\frac{1}{2})(i+j+\frac{1}{2})}{(i+j-\frac{1}{2})(i-j+\frac{1}{2})}\right] X(j\Delta) \\ &\equiv \sum_{\substack{j=n_1 \\ j\neq i}}^{n_2} b_{i,j} X_j \end{aligned} \quad . \tag{10b}$$

Note that for the case of $i = j$, it can be shown that the contribution to both of the integrals in Eq.(10) is zero.

The forcing functions for the coupled integral equations $A(\omega)$ and $B(\omega)$ in Eq.(6) are easily determined by a numerical integration over known values of the spectral components $X(\omega)$ and $Y(\omega)$. While this is a straightforward process, there is a potential problem at the high

frequency end of the spectrum, where the spectrum is truncated at the frequency $\omega = \Delta \times N_{\max}$. As discussed in [5], the accuracy of integrations of this type can be improved by adding a suitable asymptotic function to the integrand for frequencies $\omega > \Delta \times N_{\max}$ and then performing the indicated integration for the extended range. In the present study, however, this was not done: the integrations for $A(\omega)$ and $B(\omega)$ were simply truncated at $\omega = \Delta \times N_{\max}$.

Representing the required values of the forcing terms $A(\omega)$ and $B(\omega)$ in vector form, the set of coupled integral equations in (7) can be approximated by the following $(2N_p \times 2N_p)$ matrix equation:

$$\begin{bmatrix} 1 & 0 & 0 & \dots & 0 & 0 & a_{n1,n1+1} & a_{n1,n1+2} & \dots & a_{n1,n2} \\ 0 & 1 & 0 & \dots & 0 & a_{n1+1,n1} & 0 & a_{n1+1,n1+2} & \dots & a_{n1+1,n2} \\ 0 & 0 & 1 & \dots & 0 & a_{n1+2,n1} & a_{n1+2,n1+1} & 0 & \dots & a_{n1+2,n2} \\ \dots & \dots & \dots & \dots & \dots & \dots & \dots & \dots & \dots & \dots \\ 0 & 0 & 0 & \dots & 1 & a_{n2,n1} & a_{n2,n1+1} & a_{n2,n1+2} & \dots & 0 \\ 0 & b_{n1,n1+1} & b_{n1,n1+2} & \dots & b_{n1,n2} & 1 & 0 & 0 & \dots & 0 \\ b_{n2,n1} & 0 & b_{n2,n1+3} & \dots & b_{n1+1,n2} & 0 & 1 & 0 & \dots & 0 \\ b_{n3,n1} & b_{n3,n1+2} & 0 & \dots & b_{n1+2,n2} & 0 & 0 & 1 & \dots & 0 \\ \dots & \dots & \dots & \dots & \dots & \dots & \dots & \dots & \dots & \dots \\ b_{n2,n1} & b_{n2,n1+1} & b_{n2,n1+2} & \dots & 0 & 0 & 0 & 0 & \dots & 1 \end{bmatrix} \begin{bmatrix} X_{n1} \\ X_{n1+1} \\ X_{n1+2} \\ \dots \\ X_{n2} \\ Y_{n1} \\ Y_{n1+1} \\ Y_{n1+2} \\ \dots \\ Y_{n2} \end{bmatrix} = \begin{bmatrix} A_{n1} \\ A_{n1+1} \\ A_{n1+2} \\ \dots \\ A_{n2} \\ B_{n1} \\ B_{n1+1} \\ B_{n1+2} \\ \dots \\ B_{n2} \end{bmatrix} \quad (11)$$

This equation can solved for the unknown vectors of X and Y using standard matrix inversion techniques. As a check of the formulation and numerical realization of the $(2N_p \times 2N_p)$ matrix in Eq.(11), it is possible to plot the magnitude of the system matrix as a surface plot to visually look for any spatial anomalies in the structure of the matrix. Figure 4 illustrates one such plot for a 200 × 200 matrix. In this plot, the unit amplitude diagonal elements are clearly notes, as are off-diagonal elements a and b. While this is not a definite check on the accuracy of the matrix, it does show that the structure of the numerical realization of the matrix is correct.

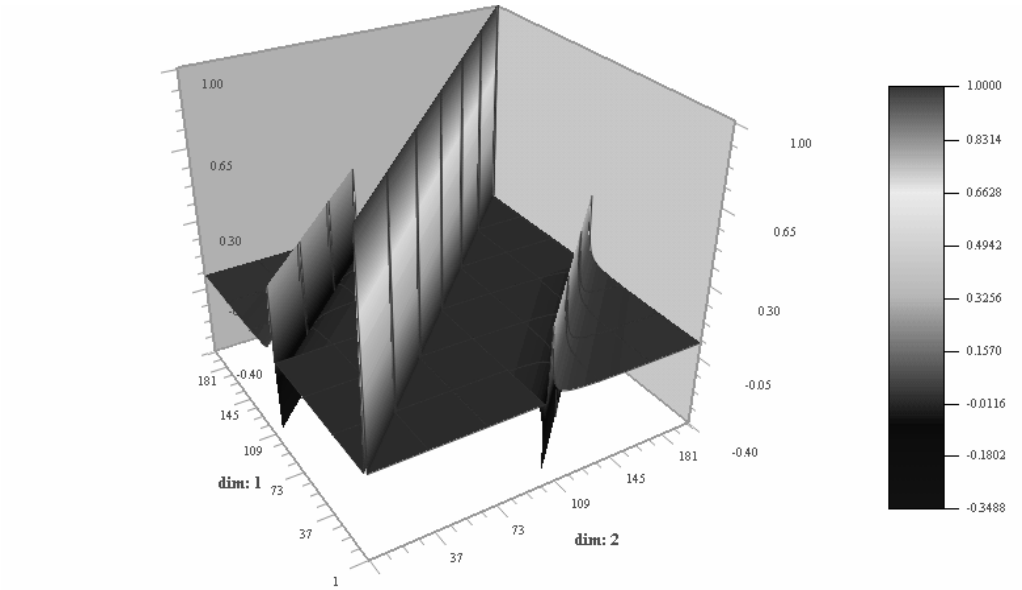

Figure 4. Visualization of the system matrix amplitudes for the Hilbert integral equation for a 200 × 200 matrix.

4. Numerical Examples

In this section, two numerical examples are provided for illustrating the application of the Hilbert integral equation (7) to non-causal spectra.

4.1 A Damped Sine Spectrum

To illustrate the use of the Hilbert integral equation for correcting an improper spectrum, let us first consider a very simple example of a damped sinusoidal waveform, as shown in Figure 5. This waveform is given by the equation

$$f(t) = A\sin\left(2\pi f_o t\right)e^{-\alpha t} \quad (for\ t > 0) \tag{12}$$

where f_o = 10 MHz, α = 10 μs^{-1}, and the amplitude A is adjusted so that the amplitude of the waveform is unity.

For this waveform, the Fourier spectrum is determined analytically as

$$F(\omega) = A\frac{\omega_o}{\left(j\omega + \alpha\right)^2 + \omega_o^2} \tag{13}$$

where $\omega = 2\,\pi f$, and $\omega_o = 2\,\pi f_o$.

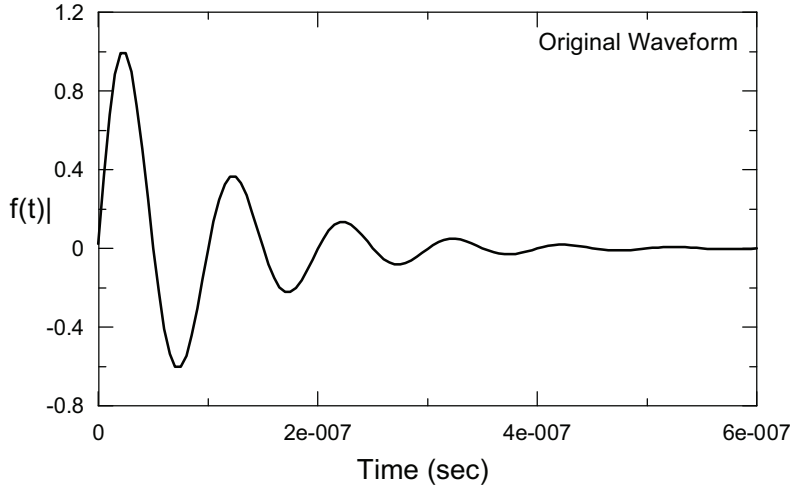

Figure 5. A damped sine waveform with frequency f_o = 10 MHz, and damping constant α = 10 μs^{-1}.

The spectrum of the damped sine is constructed over a total bandwidth of 100 MHz. In this spectrum, a region consisting of 21 frequency points (from 7.72 to 9.68 MHz) was set to an artificially low value of 10^{-9} (1/Hz). This "notch" in the waveform was designed to introduce a non-causal component to the spectrum, and to illustrate the ability of the Hilbert integral equation to reconstruct the actual spectrum in this band.

The 21-point band of frequencies resulted in a 42 × 42 matrix equation that was solved for the unknown spectral components $X(\omega)$ and $Y(\omega)$. Figure 6 presents the magnitude of the reconstructed spectrum, together with the original spectrum showing the spectral notch. Similar plots for the real and imaginary parts of the spectrum are shown in Figure 7.

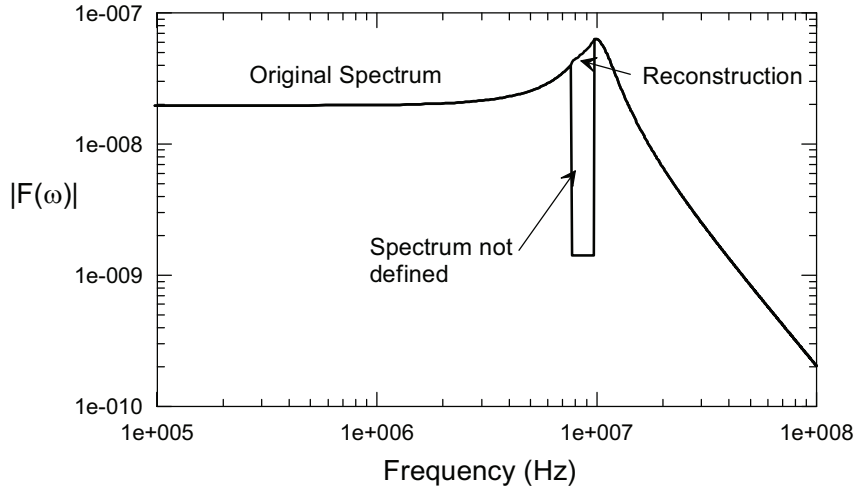

Figure 6. Plots of the original spectral magnitude of the waveform of Figure 5, showing the region where the spectrum is artificially set to a small value, and the Hilbert reconstructed spectrum magnitude.

It is interesting to examine the behavior of the reconstructed waveforms for the spectra of Figure 7. Using an inverse FFT of the spectral responses, Figure 8 presents plots of the transient responses of the original spectrum damped sine waveform of Figure 5 (dashed), the incorrect non-causal waveform and the Hilbert-reconstructed waveform. These plots show the late time responses (part *a* of the figure), together with the early time parts of the waveform (in part b). From these plots, it is clear that there is a significant non-causal component to the transient waveform (manifested by a growth of the waveform at late time). The Hilbert processing of the spectral data, however, has considerably improved the reconstructed transient response.

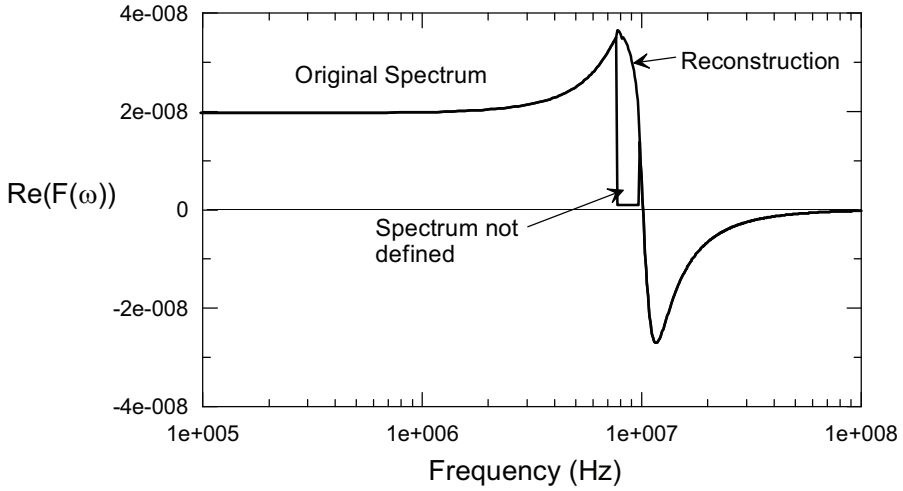

a. Real Part

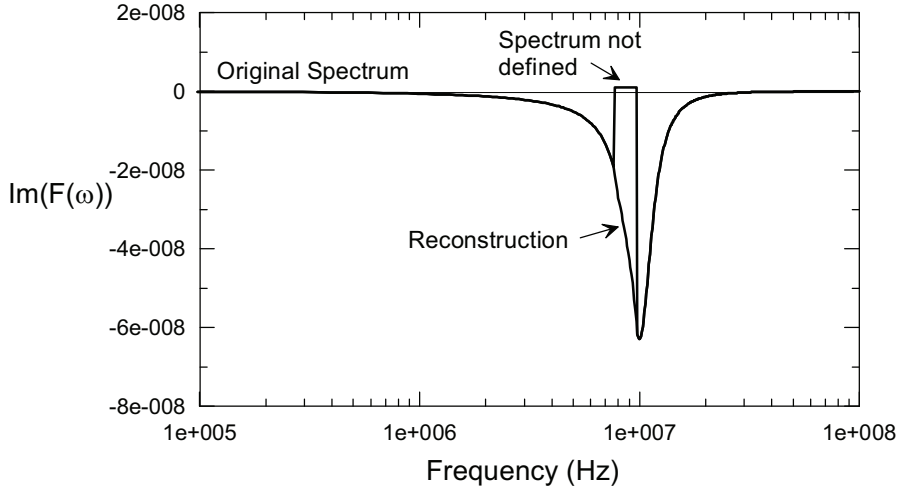

b. Imaginary part

Figure 7. Plots of the real and imaginary parts of the original spectrum for the waveform of Figure 5, showing the region where the spectrum is artificially set to a small value, and the Hilbert reconstructions.

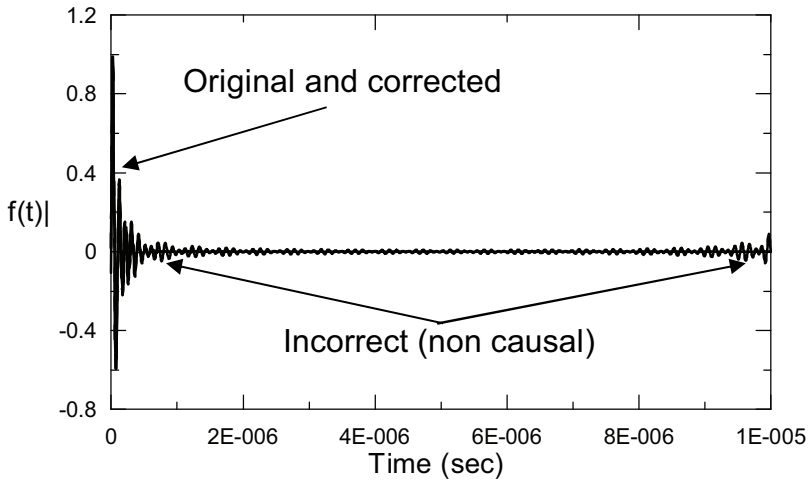

a. Late time responses

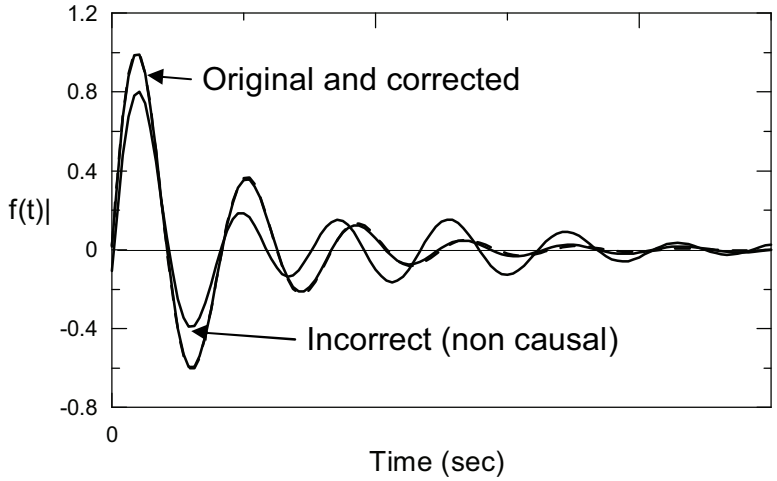

b. Early time responses

Figure 8. Plots of the transient responses of the original spectrum damped sine waveform of Figure 5 (dashed), the incorrect non-causal waveform and the Hilbert-reconstructed waveform for late time (part a) and early time (part b).

4.2 A Spectrum from a Measured Transient Response

In addition to a smooth, analytically defined waveform, it is also of interest to try the Hilbert integral equation solution on a spectrum derived from a measured transient response, which contains noise and other imperfections. A convenient waveform is the E-field produced within the ARES EMP simulator, as reported in ref. [8]. This waveform is illustrated in Figure 9, and its computed spectral magnitude is shown in Figure 10. This spectrum consists of 2049 data points, ranging from dc to about 1 GHz. Above about 250 MHz, this spectrum is dominated by noise.

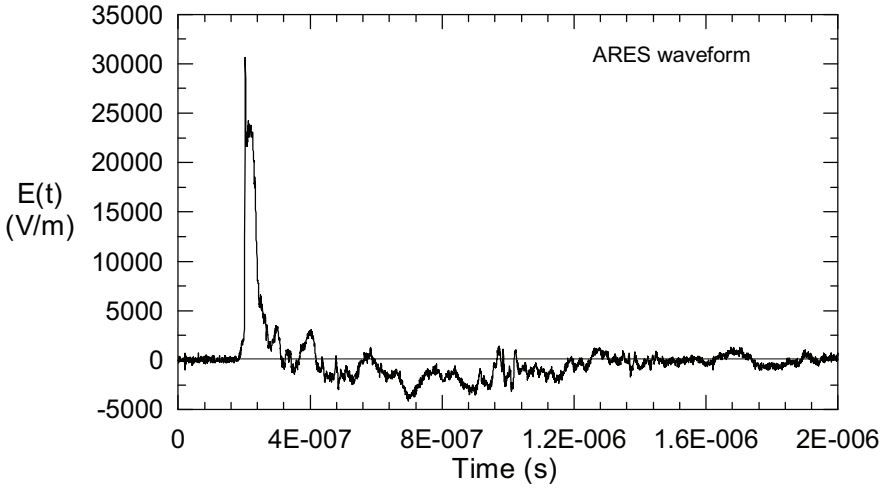

Figure 9. Plot of a measured transient waveform from the ARES EMP simulator.

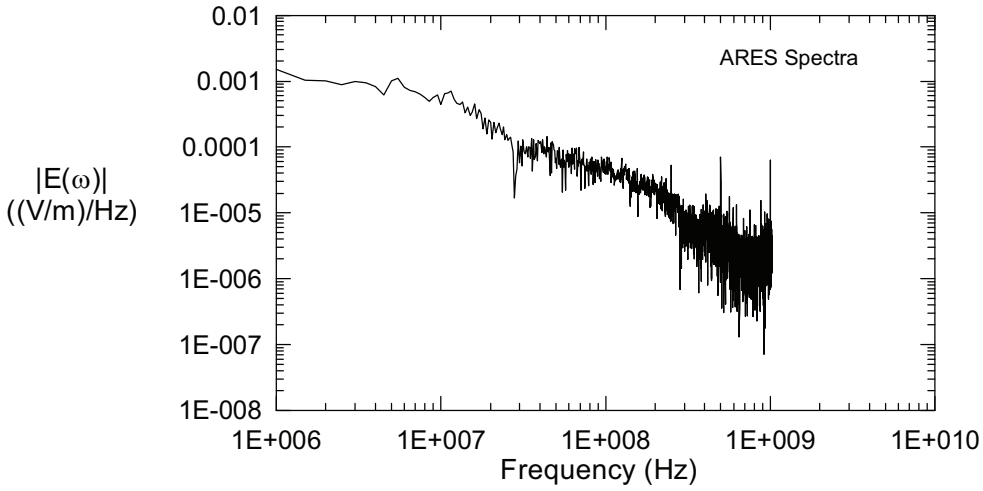

Figure 10. The spectral magnitude of the ARES waveform in Figure 9

Figure 11 shows the appropriate spectra for this waveform. The original spectrum of Figure 10 was contaminated over a range of frequencies from 39.5 to 89.0 MHz. This band contained 100 data points, and the real and imaginary parts were both arbitrarily set to 0.001 (V/m/Hz) to introduce non-causality in the response. The straight-line in Figure 11 shows this non-causal spectrum, and the Hilbert-reconstructed spectrum is also shown. Clearly in this case, the reconstructed spectrum is much smoother that was the original spectrum in this frequency band.

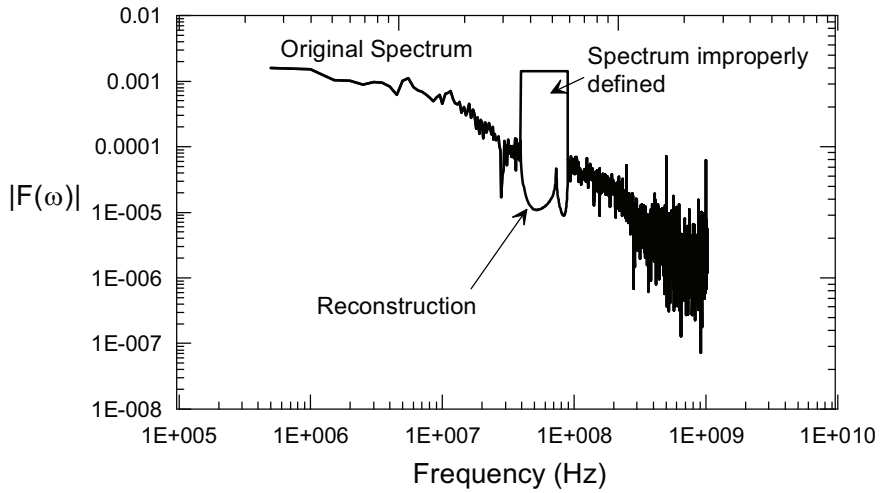

Figure 11. Illustration of the artificially modified ARES spectrum and the Hilbert reconstruction of the spectrum.

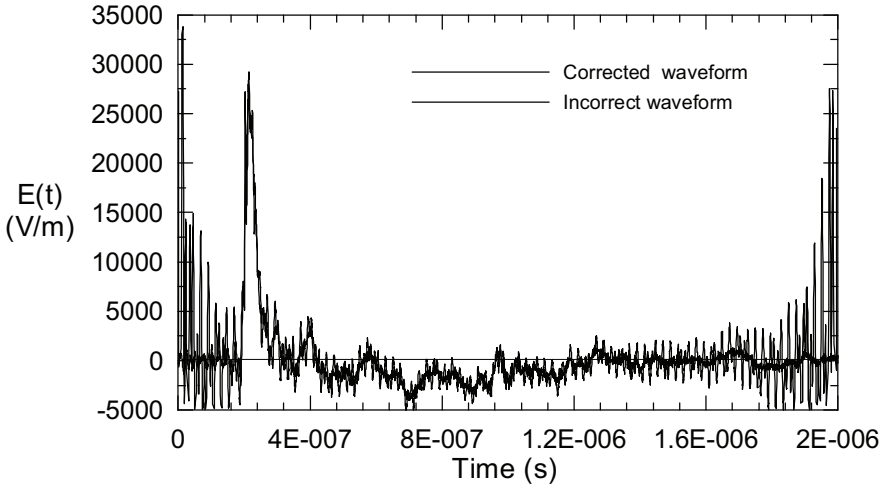

Figure 12. Plots of the Hilbert-corrected transient waveform, and the non-causal waveform resulting from the artificially modified ARES spectrum of Figure 11.

Figure 13 presents a comparison of the corrected waveform, calculated from the Hilbert spectrum, with the original ARES waveform. The agreement is quite good between these two responses, although there is a slight amount of additional noise in the corrected waveform for early time.

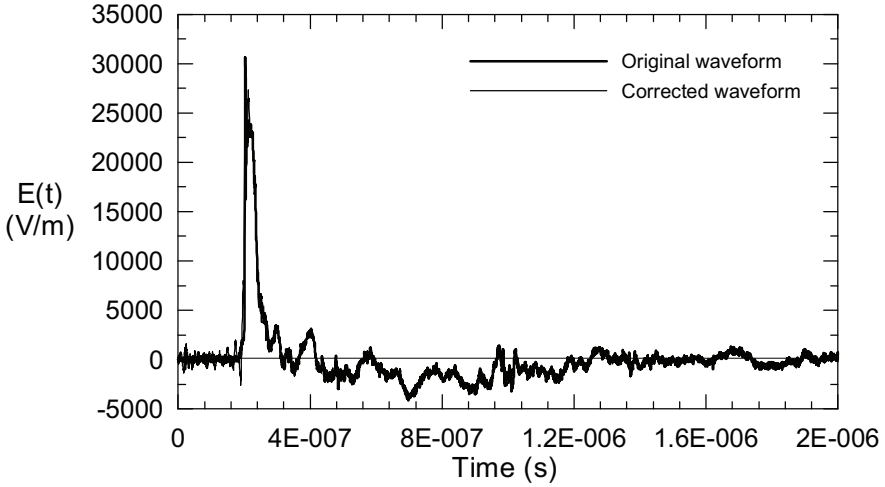

Figure 13. Comparison of the original ARES waveform and the corrected waveform.

5. Discussion

This report has shown the feasibility of using an integral equation technique based on the Hilbert transform to correct a non-causal spectrum over a limited band of frequencies. Assuming that the spectrum is causal outside this frequency band, two coupled integral equations have been formulated and solved for the unknown real and imaginary parts of the spectrum within the band. For these equations, the forcing functions are integrals of the known spectrum outside this band.

Numerical illustrations of this spectral reconstruction are provided with a simple damped sinusoid spectrum, and a more realistic spectrum arising from a measured transient waveform. In both cases, this Hilbert integral equation method gives reasonable and useful results.

While this method appears to work well for the two sample spectra used here, there are still some interesting questions about the Hilbert integral equation that fall outside the scope of this preliminary study. Perhaps most important is the issue of how large the unknown band of frequencies can be before the accuracy of the method degrades to an unacceptable level. Clearly, if frequency band is too large, there will not be enough of the original spectrum to provide for its reconstruction. This limitation on the method needs to be quantified.

Another issue of interest is to examine if this method can be applied to multiple frequency bands simultaneously. Frequently, non-causal results in a spectrum will occur in a periodic fashion in a spectrum, and removing all such effects at one time is desirable.

Finally, in an actual measured spectrum, it may not always be possible to know the exact locations of non-causal components of the spectrum. It would be interesting to examine the possibility of using this integral equation technique to estimate the regions within a spectrum where the non-causal results are occurring, and then correct the spectrum accordingly.

6. References

1. IEC 1000-2-9: “Part 4-23: Testing and measurement techniques - Test methods for protective devices for HEMP and other radiated disturbance”, 2000.

2. Papoulis, A., **The Fourier Integral and its Applications**, McGraw Hill, New York, 1962.

3. Hildebrand, F.B., **Advanced Calculus For Applications**, Prentice-Hall, Inc., 1963.

4. F.M. Tesche B. Brändli, “Suggestions for Improved CW Testing, Data Acquisition and Data Processing”, Report for DTPA Contract 109-708, Defense Technology and Procurement Agency (DTPA), NEMP Laboratory, CH-3700 Spiez, November 17, 1995.

5. Tesche, F. M., “On the Use of the Hilbert Transform for Processing Measured CW Data”, *IEEE Trans. EMC*, Vol. 34, No. 3, August 1992.

6. E. A. Guillemin, **Synthesis of Passive Networks**, Krieger Publishing, New York, 1977.

7. A. V. Oppenheim, and R. W. Schaefer, **Digital Signal Processing**, Prentice-Hall, New York, 1975.

8. Tesche, F. M., T. C. Mo, and W. Shoup, "Determination of the Electromagnetic Fields Radiated From The ARES EMP Simulator", *IEEE Trans. EMC*, Vol. 36, No. 4, November 1994.